

Analyzing the effect of landmark vectors in homing navigation

Adaptive Behavior
20(5) 337–359
© The Author(s) 2012
Reprints and permissions:
sagepub.co.uk/journalsPermissions.nav
DOI: 10.1177/1059712312449543
adb.sagepub.com



Seung-Eun Yu, Changmin Lee and DaeEun Kim

Abstract

The development of an autonomous navigating robot is a challenging task. Motivated by the performance of insects successfully returning to the nest, researchers have studied bio-inspired navigation algorithms for their potential use in mobile robots. In this paper, we analyze landmark-based approaches, especially Distance Estimated Landmark Vector (DELV), Average Correctional Vector and Average Landmark Vector methods, that use landmark vectors for visible environmental landmarks. We evaluated the homing performance of various landmark vector methods with surrounding landmarks under occlusion and found that the occluded or missing landmarks have a significant influence on the performance. We also developed a landmark vector algorithm with a visual compass that uses only retinal images without a reference compass. From our experimental results, we conclude that the DELV shows robust homing navigation performance with missing or occluded landmarks among landmark vector methods.

Keywords

Image-based navigation, landmark navigation, ALV, DELV, ACV, occlusion, visual compass

I Introduction

The development of an autonomous navigating robot is a challenging task that has been studied extensively. The robust and successful manner in which small insects navigate has attracted much attention, even though these organisms have a relatively simple nervous system with limited sensing capabilities. Many organisms have their own sets of skills for finding their way back home after foraging for food. Hymenopterans such as bees and ants go on an outward journey for food and return to the nest after their journey. Such organisms are known as central-place foragers. Among the various senses of these organisms, their navigation system involves visual (Mather, 1991), auditory (Rossier, Haeberli, & Schenk, 2000), olfactory (Papi, 1990), magnetic (Luschi, Papi, Liew, Chan, & Bonadonna, 1996) and internal motion (M. Collett & Collett, 2000) systems. It seems that navigation in these organisms relies heavily on visual information (M. Collett & Collett, 2000). Unlike other types of ants, desert ants, *Cataglyphis*, whose main habitat is the Sahara, cannot use pheromones to find their way back to the nest since pheromones evaporate in their desert habitat. Based on biological reports (Wehner & Räber, 1979), desert ants apply vision-based piloting strategies along with path integration to ultimately find their nest.

Motivated by the performances of insects successfully returning to their nest, researchers have developed

bio-inspired navigation algorithms and applied them to mobile robots. However, many of these algorithms still have problems with robot localization and determining the appropriate goal position. Development of a simple and robust homing strategy is a critical issue in this research.

Researchers conducting biological experiments have proposed that insects use a form of image matching to search for the locations of their home (Wehner & Räber, 1979; Wehner, Michel, & Antonsen, 1996). The snapshot model has been used to explain an insect's visual piloting techniques from the perspective of image matching (Cartwright & Collett, 1983). The model estimates the homing direction by comparing two 'snapshots', the current retinal image of a panoramic view and a snapshot image of the goal location. By choosing the movement that maximizes matching, i.e. minimizes the discrepancy between the two snapshots, the insects can return to the location represented by the stored image. Along with the snapshot model, researchers have also suggested that bees memorize the apparent

Biological Cybernetics Lab, School of Electrical and Electronic Engineering, Yonsei University, Shinchon, Seoul, South Korea

Corresponding author:

DaeEun Kim, Biological Cybernetics Lab, School of Electrical and Electronic Engineering, Yonsei University, Shinchon, Seoul, 120-749, South Korea
Email: daeeun@yonsei.ac.kr

sizes and bearings of landmarks observed at the target location and use them for navigation (Cartwright & Collett, 1983). There is some evidence that bees learn the distances of landmarks from the goal location, possibly through cues based on optic flow (Cheng, Collett, Pickhard, & Wehner, 1987; Esch & Burns, 1995).

A reference for orientation would also make it simpler to encode landmark information in snapshots for use in navigation. Insects are known to utilize external compass references in various forms and apply them successfully to the snapshot model (Cartwright & Collett, 1987; T. Collett, 1996). The positions of the Sun and the skylight polarization pattern can be employed as a reference (Wehner, 1997), collectively known as a celestial compass. A magnetic compass is also useful since organisms that migrate over long distances exploit terrestrial magnetism as a reference (Luschi et al., 1996). The unfailing homing ability of insects is quite interesting, and researchers have suggested that insects may possibly compose their homing strategy based on visual cues and a reference compass using the snapshot model.

Based on the visual snapshot navigation method used by insects for homing tasks, various methods for vision-based robotic homing have been suggested and implemented. These methods differ in their manner of handling an image, the type of landmarks extracted, and the scheme for processing visual information. Homing algorithms can primarily be classified into two categories: image-based methods and parameter methods.

Image-based navigation methods exploit the pixel values in a snapshot image to determine the direction home (Franz, Schölkopf, Mallot, & Bülthoff, 1998; Stürzl & Zeil, 2007; Zeil, Hofmann, & Chahl, 2003; Labrosse, 2007; Möller, 2009; Baddeley, Graham, Philippides, & Husbands, 2011). One of the most popular image-based homing methods was proposed by Franz et al. (1998). In the method, it is assumed that landmarks in a panoramic view are in the same distance from the position at which a snapshot was obtained. With this equidistance assumption, it is possible to determine how much the agent should rotate and how long it should move forward to make the view more similar to that of the goal location. The agent then predicts a possible panoramic view for every direction by 'warping' the current snapshot. Since the equidistance assumption does not correctly portray the real world, the decided homing vector does not always guarantee 100% accuracy. However, by repeatedly applying the procedure, the robot is led to the goal location in a step-wise manner. The advantage of the method is that no certain feature or landmark has to be extracted from the image. Instead, the pixel values of a snapshot image are processed to warp the image.

Parameter methods extract the landmark features from an image and select appropriate parameters that

express the characteristics of the landmarks. The simplest and most parsimonious vision-based navigation method is the Average Landmark Vector (ALV) model (Lambrinos, Möller, Labhart, Pfeifer, & Wehner, 2000). The ALV model processes an image with only a two-dimensional vector, thus requiring little memory and computation. The technique has been shown to be effective for visual navigation in both simulations and experiments on autonomous mobile robots (Lambrinos et al., 2000; Möller, 2000). In many studies, neural networks have been used to implement the ALV model (Hafner & Möller, 2001; Hafner, 2001; Smith, Philippides, Graham, Baddeley, & Husbands, 2007). In addition, a number of robotic experiments (Goldhoorn, Ramisa, Mantaras, & Toledo, 2007) have demonstrated the efficiency of the ALV approach.

In the ALV model, the ALV is computed by averaging every unit landmark vector in the omnidirectional view. Each perceived landmark vector has a unit length, and the ALV is the average of all landmark vectors in view. The agent first stores a two-dimensional ALV at the goal location. When returning to the goal location, the agent obtains a homing vector by comparing the ALV in the current view with the ALV stored earlier. The homing vector obtained from the difference between two ALVs can be determined repeatedly until the agent reaches the goal point. The ALV method requires an omnidirectional view for vector representation and an external reference compass for orientation. Studies on the behaviors of insects and their biological capabilities have shown that the ALV model may possibly be used by insects or small animals (Möller, 2001). Insects have eyes with an almost omnidirectional view and possess their own reference compass methods, such as the celestial (Wehner, 1997) or magnetic (T. Collett, 1996) compasses mentioned earlier. In addition, it is assumed that ants and bees can extract certain types of objects from a snapshot image (Cartwright & Collett, 1987; T. Collett, 1996).

While the ALV model uses the difference in the average perceived landmark vectors, the homing approaches used by Hong, Tan, Pinette, Weiss, and Riseman (1991) and Weber, Venkatesh, and Srinivasan (1999) compute a correctional vector for each landmark pair. By summing all of the correctional vectors, the agent finds the homing vector along which to move. The method by Weber et al. (1999) is similar to the ALV model in that it involves the creation of a unit landmark vector and uses correctional vectors to compute the homing vector. However, it has an entirely different computing algorithm.

Another landmark-based homing approach is the Distance Estimated Landmark Vector (DELV) method (Yu & Kim, 2011). It is possible that some insects measure the distances to landmarks using optical flow information (Esch & Burns, 1995) and optical flow has been applied to the robotic system (Schmudderich

et al., 2008) to estimate the object motion. Instead of estimating the information of a moving object, in the DELV method, the distance to static landmarks can be obtained by moving the mobile agent itself, similar to the distance estimation based on optical flow, and then the agent stores landmark vectors with distances. The landmark vectors at the goal location are stored for later comparison with those obtained at a new location. By projecting one vector set onto another (which is also the difference between the vectors), the agent computes the appropriate homing direction. The DELV and ALV methods are similar with regard to the concept of averaging the difference between landmark vectors. However, in the DELV model, distance information is encoded in the landmark vector. These landmark navigation algorithms have been tested with mobile robot experiments (Möller, 2000; Yu & Kim, 2011). It is believed that insects use a form of image matching to search for their location. The snapshot model has been suggested to explain their homing navigation behavior based on visual images (Cartwright & Collett, 1983). The landmark vector methods follow the scheme to compare the current retinal image and the stored snapshot image at home location. The DELV and ALV methods have that kind of procedure in an abstract form. However, it is still unknown whether insects use image template or parameter methods.

Vision-based navigation methods with feature extraction techniques have been developed (Chen & Tsai, 1998). Chen and Tsai (1998) suggested an incremental learning for a vision-based autonomous vehicle in indoor environments. The mobile robot uses information about vertical lines as visual features to build an environment model, and the robot locates itself based on the model consisting of the visual features of the environment. Vidal-Calleja, Sanfeliu, and Andrade-Cetto (2010) selected features in the image as landmarks to localize the robot and map the environment. Salient points as features were extracted based on a specialized saliency operator. Their work showed guidance of an autonomous vehicle using only a single camera along with real-time estimation of the motion based on the Simultaneous Localization and Mapping (SLAM) technique (Vidal-Calleja et al., 2010). On the other hand, some researchers focused on developing a navigation approach without estimating the environment accurately. Tovar, Murrieta-Cid, and LaValle (2007) presented a new framework for a mobile robot navigation with minimal requirements on sensory information. It builds a gap-based roadmap with only one sensor which tracks the directions of depth discontinuities, but without any coordinate or any localization feature. Many navigation algorithms have considered building an environmental map with visual features or other sensory information. For homing navigation, building a map is not necessary and the algorithm becomes simpler. Here, we focus on how an agent keeps

the minimal information about the environment to return home and how effectively the agent can return home. We assume that landmarks in the environment have dominant features which can be easily distinguished from the background in the visual image.

In this paper, we test various visual homing approaches. We investigate again our previous approach, the DELV method, and evaluate the homing performance under various circumstances, especially, under occlusion. The technique will be compared with the Average Correctional Vector (ACV) method suggested by Weber et al. (1999), the ALV method, and the Gradient Image Space (GIS) method by Labrosse (2007). We consider the occlusions of landmarks or missing landmarks often found in a real environment and test how those situations affect the homing performances of the methods. Here, a visual compass (Labrosse, 2006) has been applied to the landmark vector methods. Without a reference compass, visual snapshots alone can be applied for homing behavior. The DELV, ACV, and ALV methods are similar in that they represent the angular position of a landmark using a landmark vector. These methods also quantify the difference between reference landmark information and currently obtained vectors and use the information to define a homing vector. However, these landmark-based navigation approaches use different algorithms to compute the actual homing vector. In this study, we compare the performances of the methods and use the spatial error and the success rate in homing to analyze the strengths and limitations of each approach. Such an analysis will aid in the design of a robust navigation system.

Homing algorithms are first introduced in Section 2. Navigation experiments using a reference compass are presented in Section 3, while experiments conducted with a visual compass and no reference compass are detailed in Section 4. Conclusions and areas for future research are presented in Section 5.

2 Homing algorithms

In this work, we will compare landmark navigation methods, the DELV method, the ACV method, the ALV method and the GIS method. The DELV and ACV methods exploit landmark information extracted from a snapshot image, and both attempt to derive a homing vector in a step-wise fashion via appropriate landmark arrangement matching between a pair of snapshots. The differences between the two methods exist in the procedure for computing the homing vector and the criterion used for the arrangement decision. The DELV and ALV use landmark vectors, and the angular position of each vector has a directional component to the corresponding landmark. The DELV encodes the vector with distance information, while the

ALV has a unit length of vector for each landmark. As a result, the DELV can localize the agent in a reference map. The GIS method estimates the homing vector based on the pixel difference between a pair of snapshot images.

In the following sections, we describe the detailed procedure of the methods, investigate the similarities and differences between the methods, and examine the factors that affect their performances.

2.1 The DELV method

The DELV method (Yu & Kim, 2011) is a navigation approach that estimates the current location and heading direction based on the arrangement of landmark vectors. Assuming that the agent has already obtained an accurate heading direction, the homing vector is computed as in Figure 1(a), which is also described in the following equations:

$$\overrightarrow{LV_{H_i}} = (R_i, \theta_i) \quad \text{and} \quad \overrightarrow{LV_i} = (d_i, \alpha_i)$$

$$\overrightarrow{PV_i} = \overrightarrow{LV_i} - \overrightarrow{LV_{H_i}} \quad (1)$$

$$\overrightarrow{HV} = \frac{1}{N} \sum_{i=1}^N \overrightarrow{PV_i}$$

The agent first stores the landmark vectors $\overrightarrow{LV_{H_i}}$ for each landmark at the home location, where $i = 1, 2, \dots, N$ for each landmark. Each landmark vector consists of two components, the length R_i and the angle θ_i . The length of a landmark vector is the estimated distance to the landmark and the angle is the bearing relative to the heading direction of the agent. This set of landmark vectors will operate as a reference map for the subsequent homing task. At an arbitrary location, the agent perceives another set of landmark vector $\overrightarrow{LV_j}$ with the length of the vector d_i and the angle α_i . By projecting the new landmark vector onto the reference map, a projected vector $\overrightarrow{PV_i}$ can be obtained, which is shown as a black arrow in the Figure 1(a). The appropriately projected vectors would point the current location by averaging the projected vectors. Finally, a homing vector is determined with

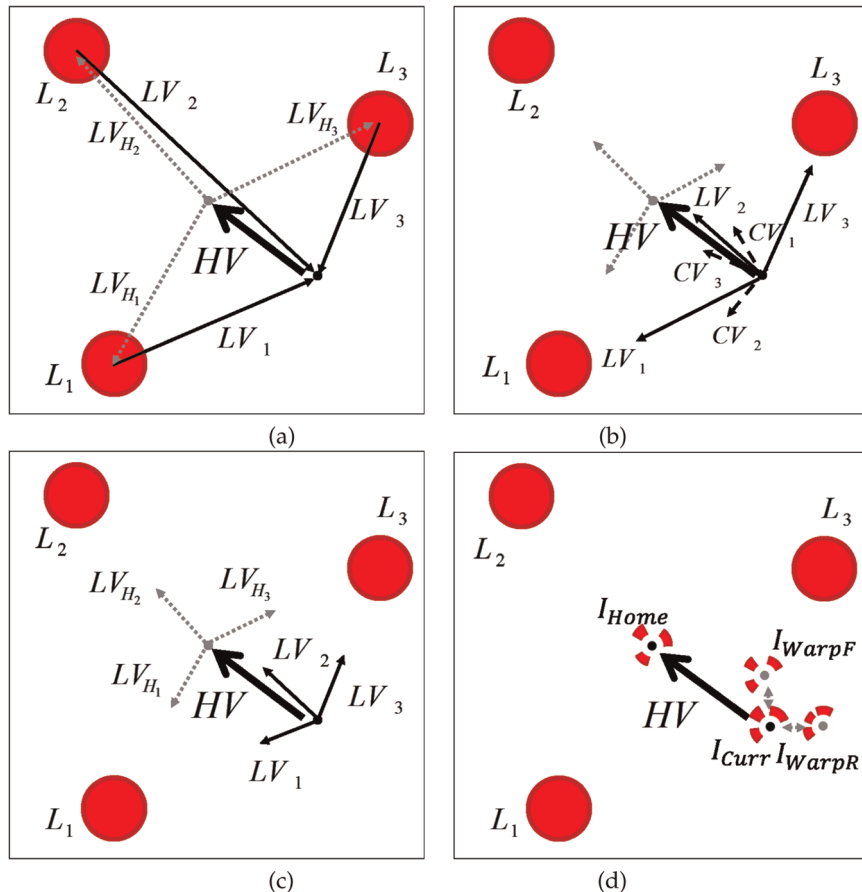


Figure 1. Graphical representation of the homing vector (HV) computation: (a) the DELV method, (b) the ACV method, (c) the ALV method and (d) the GIS method. In (b), the ACV method, CV_1 , CV_2 and CV_3 indicate the correctional vectors (dotted arrows: landmark vectors at the home location; solid arrows: inverse landmark vectors at the current location; red circles: landmarks; thick lines: homing vector).

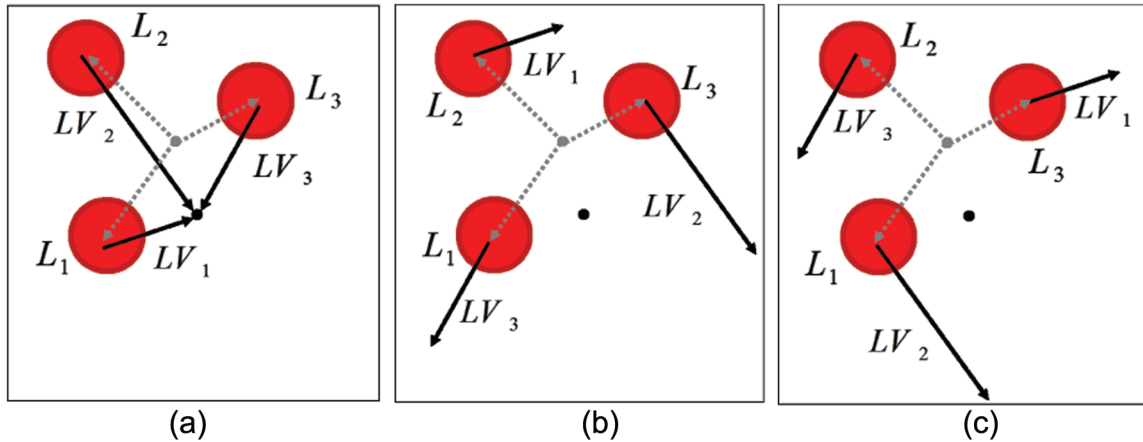


Figure 2. Projecting landmark vectors onto the reference map in different arrangement orders, and the correct order can be determined with the deviation of end points of projected landmarks ((a) is the best matching case).

the current location estimation. The remaining problem is to find the appropriate order of projecting landmark vectors.

In the DELV method, the vector set $\overrightarrow{LV_j}$ is projected onto the reference map in a rotating order. The best matching order is chosen by testing a linear order of landmark vectors. In this approach, the criterion for finding the appropriate matching order j is determined according to the deviations of the endpoints of $\overrightarrow{PV_i}$. This procedure is explained in Figure 2; $\overrightarrow{LV_j}$ is drawn with dotted arrows and the reversed $\overrightarrow{LV_j}$ are represented with solid arrows. The projecting orders j in Equation (1) can vary as shown in Figure 2(a)–(c). Based on the criterion of the deviation of endpoints of $\overrightarrow{PV_i}$, the order shown in Figure 2(a) would be chosen in this case for the correct arrangement.

The heading direction of the agent is assumed to be known for the estimation of the current location using the rotational projections of perceived landmark vectors. An estimation of the heading direction can also be obtained via landmark vector projection for each possible direction. While landmark vectors are projected onto the reference map in a rotational order, the projecting angle can vary according to the heading direction. By calculating the deviation of end points of projected vectors, the agent can estimate the current heading direction along with the current location.

2.2 The ACV method

The homing algorithm suggested by Weber et al. (1999) shows the concept of a correctional vector. A similar idea of correctional vector has been tested by Hong et al. (1991) to decide the homing direction. The ACV considers arrangement matching of landmark vectors as in the DELV method. A correctional vector of a landmark tries to improve the perceived bearing of its landmark at the current position to better match that

observed at the home location. To make the bearings of landmarks at the current position closer to the bearings of the landmarks at the home location, the robot moves perpendicularly to the current bearing of a landmark, which is not a perfect solution, but it effectively helps reducing the bearing angles of a landmark. Instead of directly exploiting the landmark vectors to obtain the homing vector, the correctional vector for each landmark is first computed. The correctional vectors are then averaged to obtain the final homing vector. Figure 1(b) and the following equation describes the concept more clearly:

$$\begin{aligned} |\overrightarrow{CV_i}| &= |\theta_i - \alpha_i| \\ \angle \overrightarrow{CV_i} &= \begin{cases} \alpha_i + 90^\circ & \text{if } \theta_i < \alpha_i \\ \alpha_i - 90^\circ & \text{if } \theta_i \geq \alpha_i \end{cases} \\ \overrightarrow{HV} &= \sum_{i=1}^N \overrightarrow{CV_i} \end{aligned} \quad (2)$$

where $\overrightarrow{CV_i}$ is a correctional vector for the i th landmark, θ_i is the angle of the i th landmark in the reference map (at home location) and α_i is the angle of the i th landmark at the current position.

Unlike the DELV method, the landmark vectors obtained by the agent in the ACV method are unit vectors. That is, landmark vectors only contain angular information, θ_i or α_i , without the additional length information of the vector. The gray dotted arrows in Figure 1(b) show the unit-length landmark vectors at home location. These are also stored in the reference map for the homing task. Then, two vectors pointing a landmark from two different snapshots are compared with each other to produce a correctional vector. The length of the correctional vector $\overrightarrow{CV_i}$ is defined as the difference in paired angles for landmark vectors, θ_i and α_i , correspondingly. Thus, if the difference between the

paired angles is large, the correctional vector becomes large, influencing the homing vector to compensate for the difference. The angle of $\overrightarrow{CV_i}$ is perpendicular to its corresponding landmark vector, and the direction is decided by comparing the angles (see Equation (2)). The criterion for choosing the appropriate matching order j is to find the minimum c according to $c = \sum_{i=1}^N |\theta_i - \alpha_j|$, which is the sum of the difference in the paired angles θ_i and α_j . In Figure 1(b), CV_1 , CV_2 and CV_3 indicate the correctional vectors that yield the homing vector \overrightarrow{HV} .

The method suggested by Weber et al. (1999) also requires a reference compass for orientation. While the DELV method is capable of estimating the current heading direction through landmark vector rotation, the reference compass information can be instead used with the DELV approach for a proper comparison with the ACV. While the two methods have significantly different types of perceived landmark vectors and different procedures to compute the homing vector, the resulting homing vectors \overrightarrow{HV} are similar in a landmark-surrounding environment, as shown in Figure 1. In such an environment, the agent can 'see' every landmark with no occlusion or perception horizon problem.

Given the above results, we could speculate that an inaccurate landmark vector set would yield error in the computed homing vector. Also, it is reasonable to assume that the different procedures for calculating homing vectors \overrightarrow{HV} would have different effects when dealing with an erroneous perceived result. We investigate the results in this paper.

2.3 The ALV method

The ALV method is one of the popular landmark vector navigation methods. Each landmark has its own landmark vector in a snapshot with the corresponding angular direction and a unit length. At home location, the agent can collect all of the landmark vectors from its surrounding landmarks, average the vectors, and store the averaged vector called ALV. The agent calculates the ALV again from the snapshot image at the current position, and compare the two ALV vectors. The difference between the two vectors can directly estimate the homing direction. The procedure can be summarized as follows:

$$\overrightarrow{LV_{Hi}} = (1, \theta_i) \text{ and } \overrightarrow{LV_{Ci}} = (1, \alpha_i)$$

$$\overrightarrow{ALV_H} = \frac{1}{N} \sum_{i=1}^N \overrightarrow{LV_{Hi}} \quad (3)$$

$$\overrightarrow{ALV_C} = \frac{1}{N} \sum_{i=1}^N \overrightarrow{LV_{Ci}} \quad (4)$$

$$\overrightarrow{HV} = \overrightarrow{ALV_C} - \overrightarrow{ALV_H}$$

where $\overrightarrow{ALV_H}$ is the ALV at the home location, $\overrightarrow{ALV_C}$ is the ALV at the current position and \overrightarrow{HV} is the homing vector.

In Figure 1(c), $\overrightarrow{LV_{Hi}}$, for $i = 1, \dots, n$, is a unit-length landmark vector for each landmark observed at home location, and the difference between the ALVs at two different positions derives the homing direction with \overrightarrow{HV} . The ALV method needs a reference compass to estimate the homing vector, since two snapshot images should have the same coordinate to compare the ALVs.

2.4 The GIS method

Unlike parameter methods, most image-based homing methods do not require additional sensor information for a reference compass. They instead use the snapshot image as a whole to compute the direction in which to move without estimating the heading direction or the correspondence between landmarks. Such a procedure is employed in the image matching (Franz et al., 1998) or GIS method (Zeil et al., 2003; Labrosse, 2007).

The visual compass method used for the estimation of the heading direction was proposed by Labrosse (2007). This method is conceptually similar to the predictive image matching approach (Franz et al., 1998), but the number of predictive images to be considered is different. Using the current snapshot, the agent creates a second adjusted snapshot images by predicting how the view might change when the agent moves one step forward or to the right. The prediction step is also called 'warping' since the process intentionally modifies the given image. For each image, the pixel difference with the reference image, i.e. the snapshot taken at the home position, is computed, and the difference indicates the physical distance between the two points (Zeil et al., 2003). Two different values from two predictive images obtained from a location one step in front of and to the right-hand side of the current position indicate the possibilities of matching with the home position from both locations. Therefore, the gradient vector based on the two difference values indicates the possible homing direction in which the agent should move; so it is called the GIS method (Labrosse, 2007).

This method uses the image matching. There are four types of images: the image at home location, the image at the current position and two warping images. We can see the principle of this method in Figure 1(d). Here I_{Home} is the image at home position, I_{Curr} at the current position and I_{warp} are the warping images from the current image. The one warping image is I_{warpR} which is a predicted image for one step right movement. The other is I_{warpF} for one step forward movement. As stated above, we compute the pixel difference between the home image and the warping images, and then we find the homing direction by comparing the differences with two warping images:

$$\begin{aligned}
 & \text{pixel difference between home and current} \\
 & \text{position images : } \text{diffC} \\
 & \text{pixel difference between home and right} \\
 & \text{warping images : } \text{diffR} \\
 & \text{pixel difference between home and forward} \\
 & \text{warping images : } \text{diffF} \\
 \text{moving direction} & = \text{atan2}(\text{diffF} - \text{diffC}, \text{diffR} - \text{diffC}) \quad (5)
 \end{aligned}$$

The image matching method suggested by Franz et al. (1998) uses a warping image for each sampled angle, often producing many predicted images, while the GIS method uses warping images with only forward and right movement. Therefore, this method is more efficient to determine the homing direction. However, calculating the pixel difference between a warping image and the home snapshot image needs much computation time, and it takes longer time than the parameter methods including the DELV, ACV and ALV methods.

2.5 Computational complexity

The landmark vector methods such as the DELV, the ACV and the ALV often take shorter time than image warping methods. The image warping method attempts to match the whole images taken at two different locations, that is, at home location and at the current position. The computation time is proportional to the number of pixels to be compared as well as the number of warping images. The GIS method needs two warping images for forward movement and right movement from the current position, and so it takes computation time to produce two warping images as well as compare the warping images and the home image. If the image warping method considers a set of covering distances to be warped, instead of a fixed distance, the computational complexity of the method can be represented as $O(m * w * h)$ where m is the number of testing distances, and w and h are the width and height of the panoramic image, respectively.

In contrast, the ACV, DELV and the ALV take time to choose landmarks in a snapshot and determine the angular position of landmarks. The landmark vectors at home location can be calculated in advance, and the methods take time of extracting landmark features. The ACV and the DELV execute the landmark arrangement matching process of two sets of landmarks obtained at home location and the current position. The arrangement matching process takes time $O(n^2)$ where n is the number of landmarks. In addition, the DELV needs to estimate the distance to each landmark. The agent can move forward and then determine the distance based on optical flow, unless other distance sensors such as a laser sensor or an ultrasonic sensor are available. The distance estimation time should be added for the DELV

model. The above estimations assume that the reference compass is available. Without a reference compass, each method needs to estimate the current orientation of an agent in the reference coordinate.

In our experiments, an omnidirectional snapshot image is represented as an one-dimensional array of binary value, which has 360 pixel values. Landmarks or objects are encoded as value one in the snapshot image and empty space as value zero. Landmarks are extracted from binary images and then the angular position of landmarks are estimated. Here, the feature extraction process to find landmark vectors is rather simple. For a one-dimensional snapshot, the computational complexity of the ACV, DELV and ALV is $O(w)$ for landmark extraction where w is the width of a panoramic image. The time complexity for the distance estimation is also $O(w)$. The whole procedure of the DELV algorithm takes time $O(w + n^2)$, where n is small compared with w in an image. Without distance estimation, the same level of computation time can be expected for the ACV method. The ALV method takes $O(w)$ time, mostly for the landmark extraction.

2.6 Navigation and occlusion

In the previous subsections, the procedure for obtaining the homing vector when the agent can perceive every landmark without an occlusion was explained. Occlusion is the phenomenon that the agent loses the landmark information in the arrangement of landmarks. For example, the agent initially perceives landmarks surrounding the home location, and when the agent moves sufficiently far from home, or experiences noisy sensor readings or small contrast image readings, it may encounter occlusions or the disappearance of landmarks; some landmarks may be hidden by other landmarks or background objects. In addition, relatively small-sized landmarks may be invisible in a noisy environment. Here, we assume that all of these cases are classified as occlusions.

In our simulation experiments, some landmarks may be intentionally removed to monitor the effect of occluded landmarks. A landmark can be occluded by background objects or other landmarks. If a landmark is hidden by another, then the two landmarks look merged into one and then it appears as a single landmark. In real environmental images, some landmarks may not be observed by noise or similar colors with the background. This kind of aliasing can happen in reality, and it influences the homing navigation performance with wrong information about landmark distribution.

Figures 3 and 4 illustrate the procedure for a situation in which one landmark is missing from view. Rotational landmark vector matching for deciding the best pairings is shown in Figure 3. As mentioned above, we only consider n possible cases in this approach for n landmarks. The same projecting procedure as described

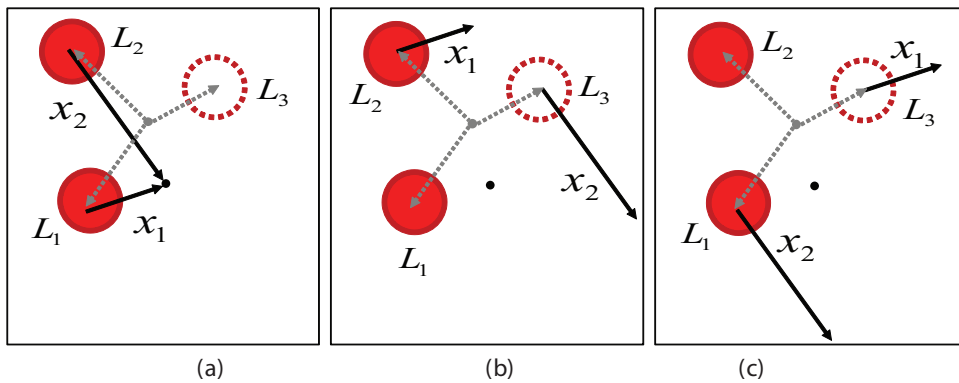


Figure 3. The arrangement matching procedure used in the DELV method for projecting landmark vectors onto the reference map when one landmark (L_3) is missing. Using the same rotational arrangement matching, the best matching order (a) is chosen.

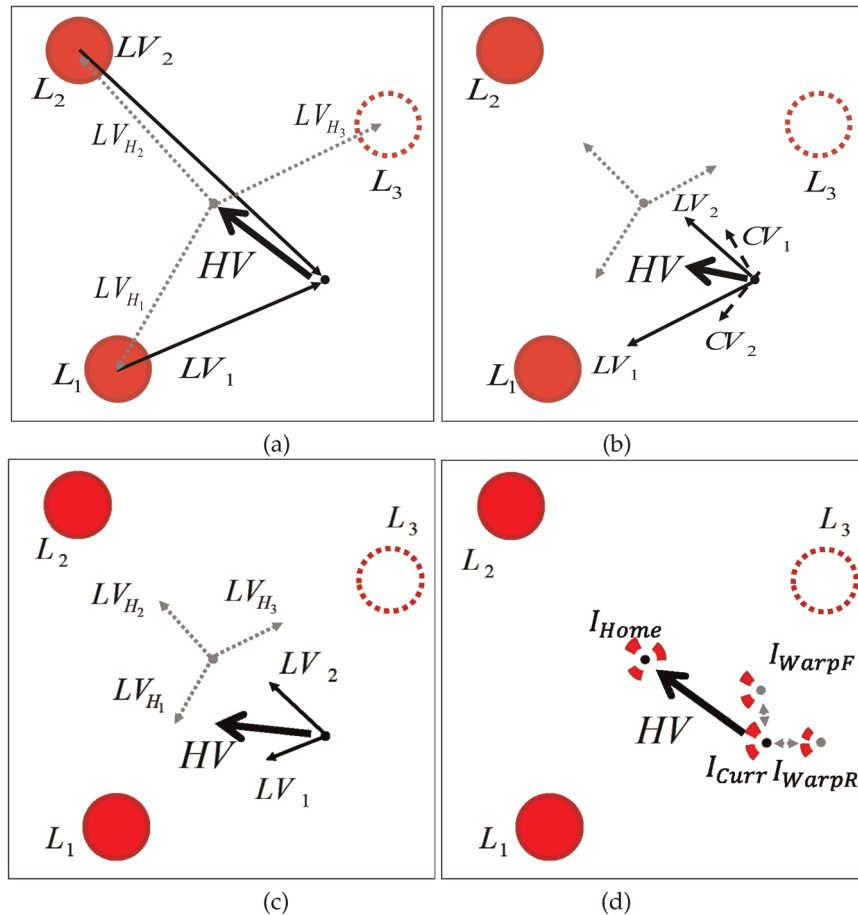


Figure 4. Homing vector (HV) computation when L_3 is occluded in (a) the DELV method, (b) the ACV method, (c) ALV method and (d) GIS method. Here, V_1 , V_2 and V_3 indicate the correctional vectors (dotted arrows: landmark vectors at the home location; solid arrows: landmark vectors at the current location; thick lines: homing vector).

in Figure 2 is applied in this situation. Since three landmarks are perceived at the home location, it is assumed the agent observes only two landmarks at a specific position. Two landmark vectors LV are projected to compute the deviation of the end points of the vectors. As a result, the procedure in Figure 3 can be used to

determine the best matching order for the method even though there is a lack of information. A similar procedure can be performed for the matching order process of the ACV method and the ALV method.

Shown in Figure 4 is the homing vector computation procedure under the assumption that the best order of

landmark pairing has been obtained for both methods. In the DELV method, if the agent correctly determines the matching order for LV_{Hi} and LV_{Ji} , the homing vector estimation becomes quite simple. In the ACV method described in Figure 4(b), the agent obtains only two correctional vectors, CV_1 and CV_2 , with the accurate pairing function. Combining two correctional vectors, the agent obtains the homing vector. In Figure 4(b), the homing vector does not directly point toward the home location. However, since all of the methods are to be applied repeatedly throughout the homing procedure, as long as the homing vector does not diverge significantly from the desired direction, it could possibly lead to the goal location. It seems that, with appropriate landmark vector matching or image matching, the methods still result in successful homing. Therefore, deciding the pairings of landmarks or landmark vectors in the reference map and in the current view is a critical step in the computation of the homing vector in the landmark vector approach.

Based on the above concept, we assess the effect of occlusions or missing landmarks with simulations in the next section.

3 Experiments with a reference compass

In this section, the results obtained with all of the methods, DELV, ACV, ALV and GIS method, for robotic experiments with various environments or configurations are presented. By comparing the experimental results, we expect to be able to analyze the characteristics of each method in certain environments. Here, we set the same conditions for all of the methods. The DELV model can be operated with or without a compass sensor. When there is no reference compass available, the agent can estimate the heading direction through the landmark vector rotation process. However, since the ACV and ALV methods require compass information to compute the homing vector, the same conditions of a reference compass were used for all of the methods. In addition, Weber et al. (1999) have suggested various landmark vector pairing algorithms in previous research. However, in this work, we limit the possible pairing function to only linear rotation of the landmark vectors for all of the methods except the GIS method.

For each method, an analysis of the computed homing vector and an examination of the homing path were conducted. While the homing vector analysis focuses on the homing direction at an arbitrary point, an analysis of the homing path would yield perspectives on the consecutive movements.

Vector maps graphically represent the computed homing vector results for a set of grid points. The vector maps for the DELV, ACV, ALV and GIS methods are shown in Figure 5. Four black circles are landmarks

in the environment, and the point located at the center at (500,500) is the home location. The arrows indicate the homing direction, that is, the decided direction of movement at each location in the map. As shown in the figure, the arrows in four methods successfully converge toward the home location.

For a comparison in various environments, three types of landmark environments were constructed. All three environments contain four cylindrical landmarks but with different sizes and angles. The first environment is at the first column of Figure 5. Four landmarks are asymmetrically surrounding the home location at (500,500) in *environ#1*. The second environment *environ#2* has a uniform distribution of landmarks (see the second column of Figure 5). Since there are four landmarks surrounding the home location, the bearing angle of each landmark, as seen at the goal location, differs by 90° from that of its neighboring landmark. The third environment also contains an asymmetric distribution of landmarks. As seen in the third column of Figure 5, all four landmarks in the environment are positioned to the left of the home location. These tests in various environments will assess the effect of landmark distribution.

We define the catchment area as a region from which an agent or a robot can ultimately return to the goal point or nest. The actual homing ability can be affected by various conditions such as trap points, attractors and obstacles. That is, starting from a point outside of the catchment area, the agent would not be able to reach home. Instead, the agent would be stuck in some single location or would circle around a certain region, known as a 'trap point'. Even though the vector map results reveal a sufficiently low number of error points, even a few trap points can keep the agent from moving toward the goal location and thus, degrade the homing performance. The squared area in Figure 5 indicates the catchment area; if the agent starts from this area, it can successfully return home. The DELV method shows 92% of the catchment area, while the ACV and ALV displays 100% of the catchment area for the environment *environ#1*. The reason for the 8% failure with the DELV method is related to the existence of several trap points not in the landmark-surrounding area. The GIS method has smaller catchment area of the environment, and the catchment area often belongs to the landmark-surrounding area. If the distance to each landmark could be estimated correctly in the DELV system, the performance would be the same as the ALV. Here, the DELV system estimates the distance using the amount of shift of a landmark when the agent moves forward. If a landmark is occluded by another, the distance estimation becomes inaccurate for both landmarks, which influences the homing performance.

The angular error graphs corresponding to the vector maps in Figure 5 are shown in Figure 6. We divided the homing vector result into three categories

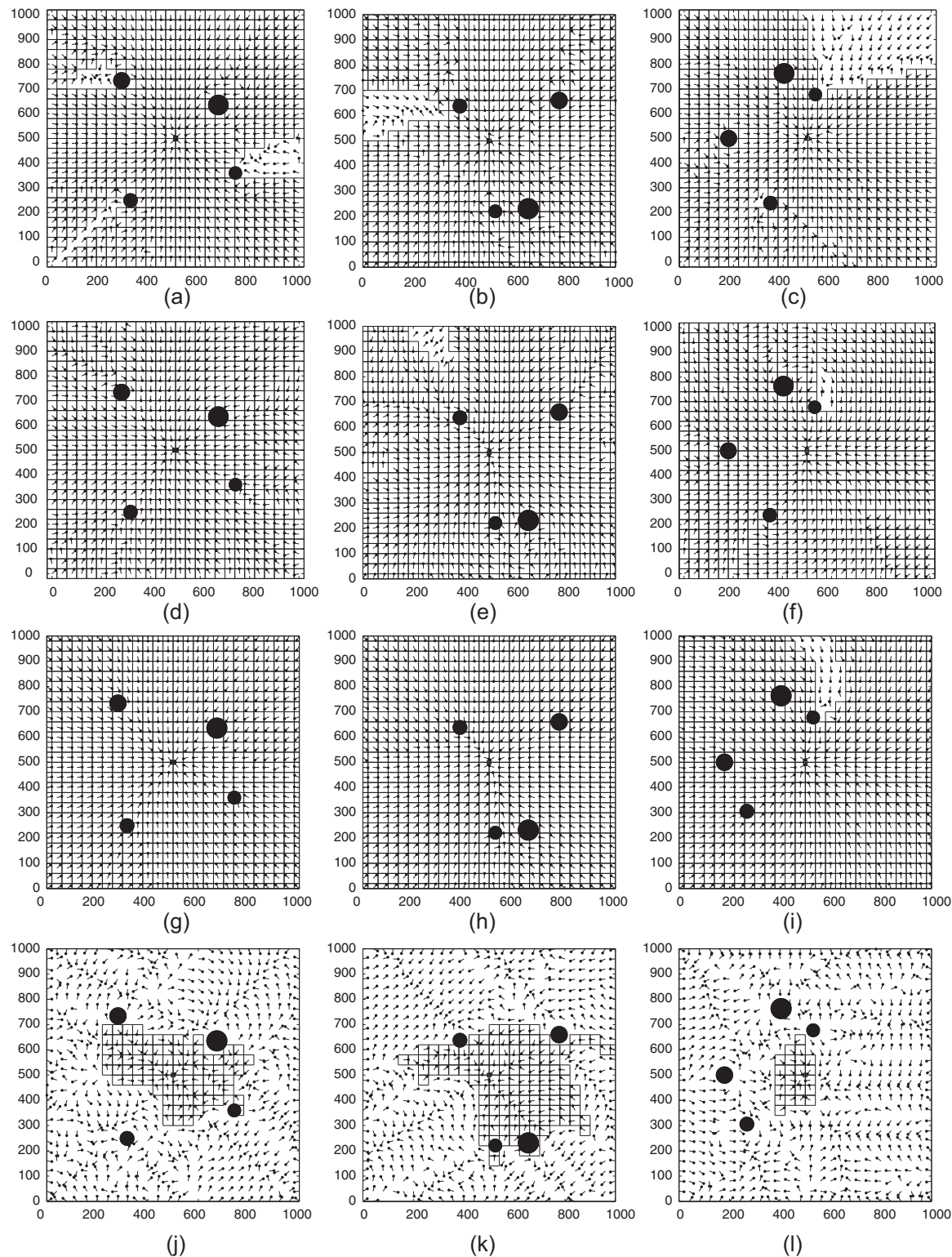


Figure 5. Vector maps with catchment area (boxed region) for (a)–(c) the DELV method with compass, (d)–(f) the ACV method, (g)–(i) the ALV method and (j)–(l) the GIS method in each environment.

based on the angular error, defined as the difference between the decided homing direction and the angle of a desired straight line from the current location to the home location. The points indicated with dots have small errors less than 45°, while the points

represented as stars have errors greater than 45° but less than 90°. Finally, points with angular errors greater than 90° are indicated with a triangle. The error graphs in Figure 6 show the angular error pattern in the spatial map. It seems that the DELV, ACV

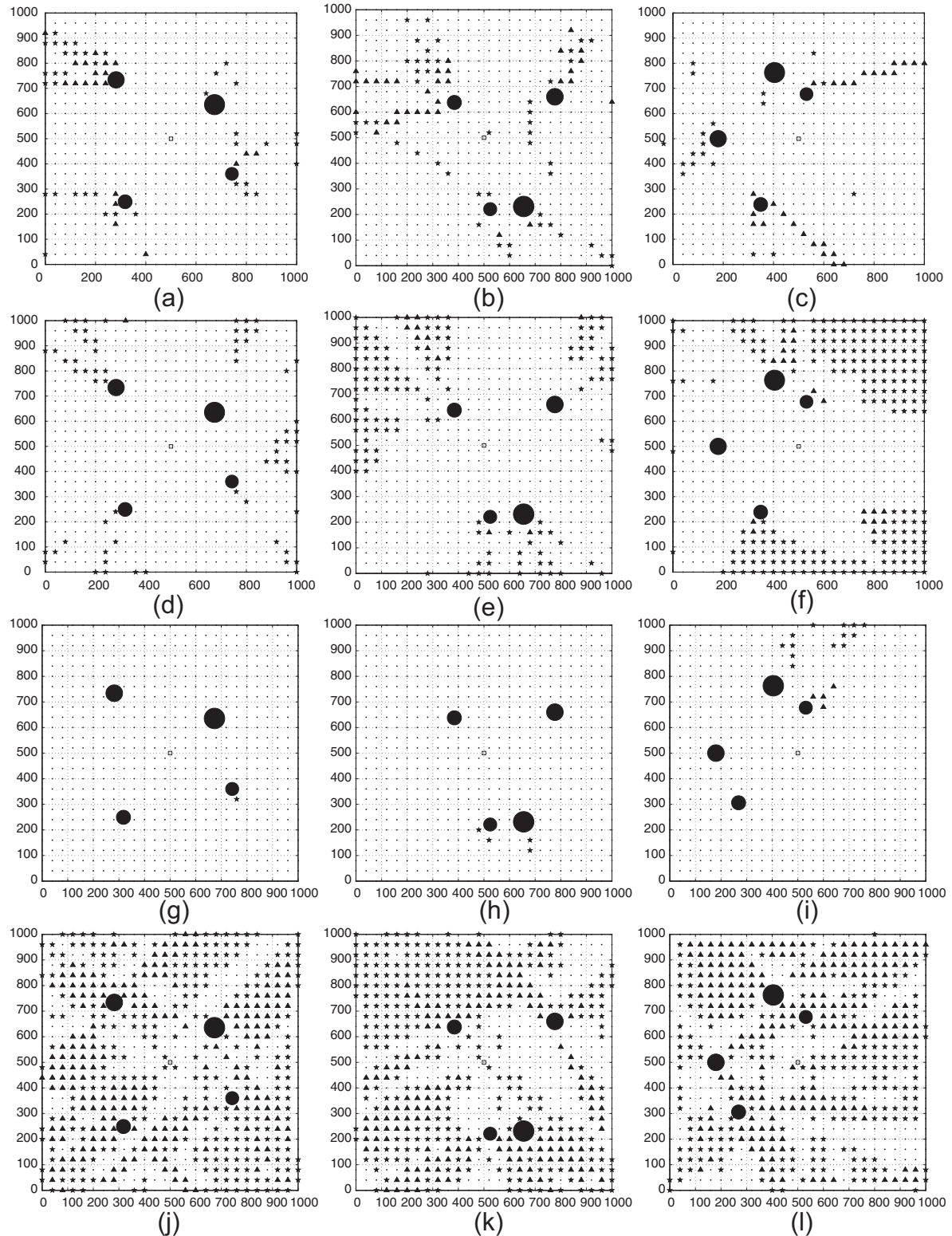


Figure 6. Points of error in the homing vector, where the marker of each point indicates the amount of angular error (dot: less than 45° ; star: between 45° and 90° ; and triangle: greater than 90°): (a)–(c) DELV method with compass, (d)–(f) the ACV method, (g)–(i) the ALV method and (j)–(l) the GIS method in each environment.

and ALV methods work effectively in all three of the environments, while the GIS method has worse performance.

The angular errors for the results in the six vector maps of Figure 5 are compared in Figure 7. The graphs labeled *D* were generated from the DELV results, while

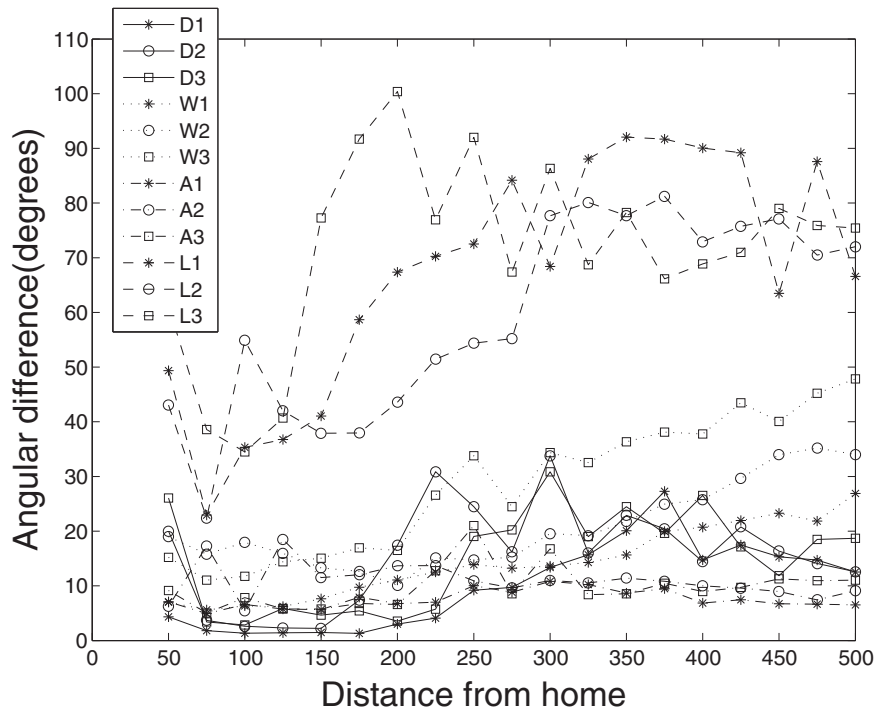


Figure 7. Error graphs for the DELV (D1, D2, D3), ACV (W1, W2, W3), ALV (A1, A2, A3) and GIS method (L1, L2, L3) results in three different environments (numbers indicate the environment type).

the graphs with a W were obtained using the ACV method, A the ALV method and L the GIS method. The number following each letter refers to the environment number (1, 2 or 3). Overall, the angular errors of the DELV method are slightly smaller than the ACV and ALV method, and much smaller than the GIS method. In Figure 7, the ACV method and the GIS method exhibits relatively large errors in the third environment. Using all of the results, the ACV method often shows an increased error rate in an asymmetric environment. Landmark arrangement matching only covers n possible matching cases with the rotational matching method, where n is the number of landmarks. With the same n candidates in the matching procedure, the DELV method successfully determines the homing direction in a robust manner in the environments. For example, the results in Figure 5(a), (d), (g) can be compared. Their corresponding error graphs are $D1$ and $W1$ in Figure 7. Upon comparison of the three graphs in Figure 7, the error graph of the DELV method is found to be slightly smaller than that of the ACV and ALV methods. However, a different perspective is shown in Figure 5(a). In Figure 5(a), a collision of arrows is observed at points (840, 440) and (280, 240). The colliding vectors indicate that if the agent enters this point, it would continually moves around the point but would not escape from the area. Therefore, the error rate in the vector map cannot effectively express the homing ability or the overall spatial performance. Here, we can test the homing performance of each method based on

the percentage of the catchment area, as shown in Figure 5.

In general, the GIS method shows lower performance than the others in our experiments. As mentioned earlier, this method is a kind of image matching method. Its performance is outstanding in the real environment including natural background images. The image warping method uses the whole snapshot image. If it includes a variety of background images, it could be helpful to match two snapshots. In our experiments, the background is simply set and the advantage of the image warping method may not be well reflected. Thus, we cannot assert that the parameter methods using the DELV or ACV method outperform the GIS method in real environment. However, the above results show a potential of landmark vector methods for homing navigation. If the landmark features could be identified, or similar features can be found in a pair of snapshots, the methods show good performance of estimating the homing direction.

3.1 Effects of occlusions

To further investigate the characteristics of the homing algorithms, we set up artificial occlusions or missing landmarks in the environments. The term occlusion indicates a situation in which a landmark cannot be seen due to other landmarks or objects. With the presence of several landmarks in an environment, there will be some occlusion regions, and more landmarks tend to

produce more occlusions. In real-world robotic experiments, occlusions can also exist due to many other factors, such as passing humans, the lighting condition, or faults in the feature or landmark extraction procedure. However, in this section, we simulate occlusions so as to evaluate their effects and examine the performance of each method in such a situation.

Occlusions or missing landmarks were simulated by removing some landmarks when a robot attempted to perform homing navigation. As a result, the agent may not be able to see the occluded landmarks. Using this situation, we actually create a discrepancy between two snapshots and, thus, can analyze the performance of each method in the presence of an occlusion.

The landmark simulation results in environment #1 are shown in Figure 8, and the results are displayed with angular errors. The results with none of the landmarks being intentionally occluded are shown at the first column of Figure 8, while the second column has one occluded landmark and the third column has two occluded landmarks. The upper three figures are the results obtained with the DELV method, while the second three graphs reveal the results attained with the ACV, the third with the ALV, the fourth with the GIS method. The results in Figure 8 show the change in the performance of each method depending on the number of occlusions. As the number of occluded landmarks increases, all methods show increasing error. However, the ACV and ALV methods show a much more rapid increase in error compared with the other two methods. That is, they are more sensitive to snapshot discrepancies when determining the homing vector. More detailed numerical results are given in Tables 1 and 2. The error point rates for environments #1, #2, and #3 are shown in Table 1. For each method, the error point percentage is shown along with varying numbers of occluded landmarks. The no occlusion column corresponds to the vector map results and the angular error graphs in Figures 5 and 7, respectively; the *environ#1* row shows the numerical results from Figure 8.

The vector map results when there are one or two occlusions in the environment are shown in Figure 9; the results of the DELV, ACV, ALV and GIS method are given. While Figure 9(a) and (c) are identical to the vector maps in Figures 5(a) and (c), Figures 9(b) and (e) have one landmark missing and Figures 9(c) and (f) have two landmarks missing. We only show *environ#1* results, although we tested three different environments. Upon comparison of Figure 9(a) and (d), the ACV method is found to yield a larger catchment area than does the DELV method. This is also true in the environment with one occluded landmark; the catchment area percentages are 85% and 93% in Figure 9(b) and (e), respectively. However, the percentage of catchment area in both methods severely decreases as the number of occluded landmarks increases. This may be the

natural consequence of the angular error graphs shown in Figure 7.

The obtained catchment area rates for environments #1, #2 and #3 with different landmark distributions are shown in Table 2. For the environment with no occlusions, the ACV method yields a larger catchment area than does the DELV method. The ACV method shows 100% of the catchment area for both the first and second environments and 98% of the area for the third environment, while the DELV method shows about 85–97% of the catchment area for the three environments. An analysis of the results reveals that landmark occlusions affect the performances of the navigation algorithms and increase the angular error of the overall region. The occlusions also shrink the catchment area, as shown in Table 2. The noticeable trend shown in the table is that the catchment area generated with the ACV method shrinks more rapidly than that produced with the DELV method. As a result, the catchment area of the DELV method exceeds that of the ACV method when two of four landmarks are occluded in the environment. This indicates that the ACV method, despite its large catchment area in the environment with no occlusions, is once again vulnerable to the occlusion problem, compared with the DELV method. An examination of the vector map results reveals that the difference between the vector maps obtained with each method can be attributed to the existence of the vector flow with an attractor to the home location or the trap point. This flow was one of the reasons for an increase in the angular error but the flow may possibly result in successful homing.

We tested all of the methods for several different environments with varying numbers of landmarks. Figure 10 shows the environments. For the test, we removed landmarks one by one, and observed the performance degradation depending on missing landmarks. Through the experiments, we wished to find which method shows robust homing navigation performance under occlusion or missing landmarks. The results in various environments with different landmark numbers are shown in Tables 3 and 4. Each environment almost has a uniform distribution of landmarks. In the environment with varying numbers of landmarks, the DELV shows better performance with respect to the angular error and the catchment area. Interestingly, we found that with the DELV method, the agent almost succeeds in returning home in the landmark-surrounding area, even if a few landmarks are missing. If the agent is far away from the home location, it may more often experience being stuck at trap points (see Figure 9). Figure 11 shows the angular errors in the environment with a uniform distribution of six landmarks. When three landmarks are missing or occluded, the figures still show good performance with the DELV method.

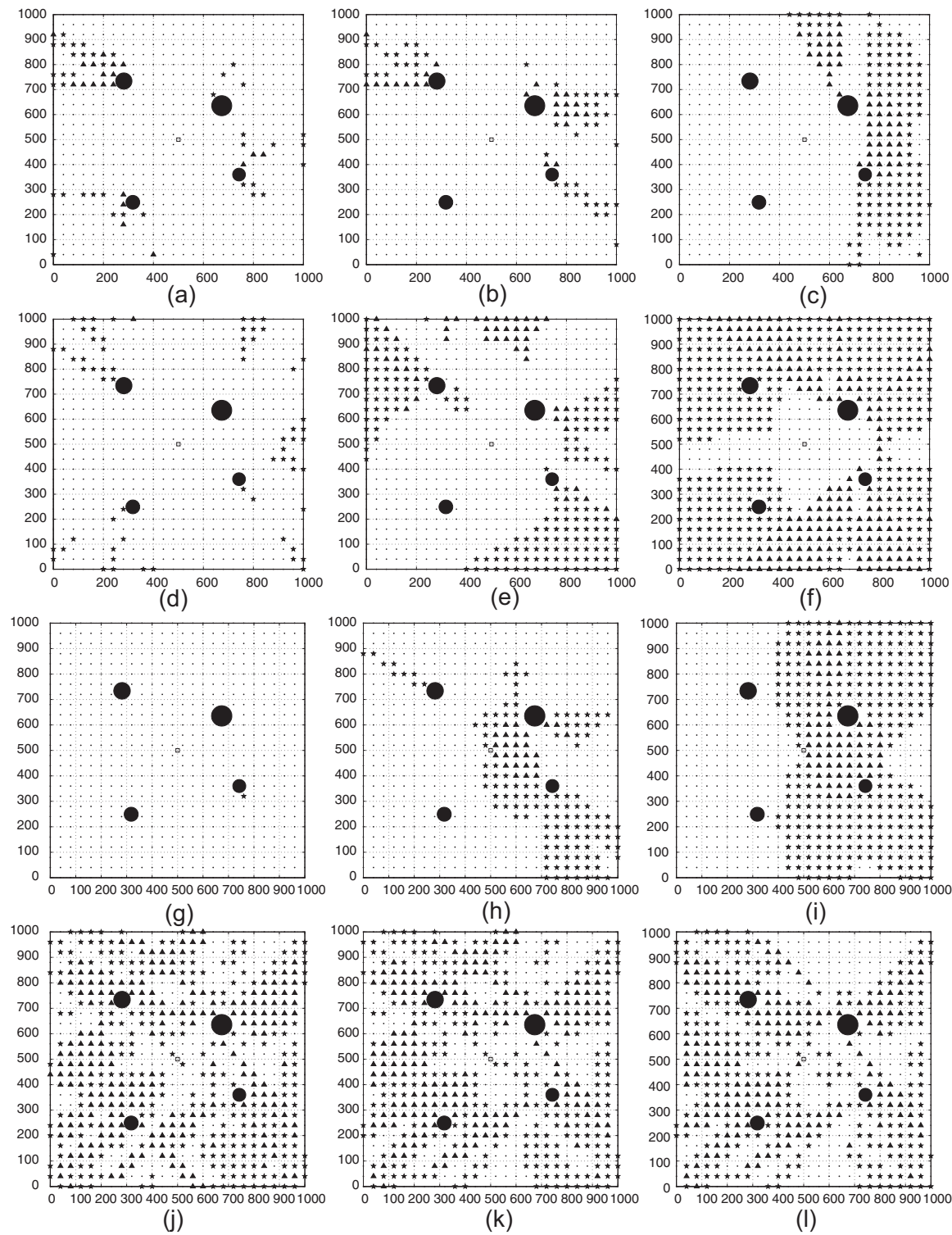


Figure 8. Graphs showing error points as the number of occluded landmarks increases from (a),(d),(g),(j) zero to (b),(e),(h),(k) one and (c),(f),(i),(l) two using the (a)–(c) the DELV method, (d)–(f) ACV method, (g)–(i) the ALV method and (j)–(l) the GIS method (dot: less than 45°; star: between 45° and 90°; and triangle: greater than 90°).

In this section, the characteristics and advantages of the landmark-based methods in certain environments and situations were investigated, with primary focus on the homing vector and the rate of successful homing.

When comparing all of the methods, the DELV method shows a much smaller error rate in the vector map results. The DELV method also tolerates the occlusion problem with better performance, even if the method

Table 1. Error point rate (%) for each environment with a different landmark distribution

| Occluded # | None | 1 | | 2 | |
|------------|------|---------|---------|---------|---------|
| | | e > 45° | e > 90° | e > 45° | e > 90° |
| Environ#1 | DELV | 5.73 | 3.02 | 6.79 | 3.62 |
| | ACV | 9.65 | 0.15 | 25.34 | 7.39 |
| | ALV | 0.15 | 0 | 18.40 | 3.77 |
| | GIS | 34.41 | 30.92 | 38.16 | 27.75 |
| Environ#2 | DELV | 7.08 | 4.82 | 9.04 | 4.52 |
| | ACV | 18.67 | 1.66 | 44.28 | 15.51 |
| | ALV | 0.6 | 0 | 34.53 | 6.33 |
| | GIS | 39.46 | 23.49 | 41.27 | 16.27 |
| Environ#3 | DELV | 3.78 | 5.59 | 4.23 | 3.63 |
| | ACV | 41.09 | 1.96 | 42.75 | 10.73 |
| | ALV | 1.96 | 0.6 | 24.7 | 8.76 |
| | GIS | 28.7 | 30.97 | 34.29 | 28.25 |

Table 2. Catchment area rate (%) for each environment with a different landmark distribution

| Occluded # | none | 1 | 2 |
|------------|------|-------|-------|
| Environ#1 | DELV | 92.01 | 85.95 |
| | ACV | 100.0 | 93.79 |
| | ALV | 100.0 | 17.60 |
| | GIS | 12.87 | 27.07 |
| Environ#2 | DELV | 95.27 | 49.56 |
| | ACV | 97.78 | 53.99 |
| | ALV | 100.0 | 17.46 |
| | GIS | 19.82 | 19.67 |
| Environ#3 | DELV | 86.24 | 85.95 |
| | ACV | 98.67 | 45.34 |
| | ALV | 96.01 | 7.40 |
| | GIS | 3.55 | 2.66 |

shows increased error rates as the number of occlusions increases.

4 Experiments without a reference compass

Many robotic navigation methods, such as the ALV and the ACV models, require reference compass information. However, in indoor environments, difficulties in the use of a magnetic compass or other reference compasses may be encountered. Thus, a navigation method that is independent of the reference compass is advantageous. Several visual homing methods determine the homing direction without compass information through the use of a snapshot image. The image distance computed by the pixel differences between two snapshot images is proportional to the physical distance between the locations where the snapshots were taken (Zeil et al., 2003). Using a similar concept, the heading direction can be computed via the rotational matching of two snapshots, a method known as ‘visual

compass’ (Labrosse, 2006). As a result, the compass sensor can be eliminated.

4.1 Visual compass method

The visual compass method has been suggested to estimate a heading direction based on snapshot images (Labrosse, 2006, 2007). The method computes the discrepancy between a pair of omnidirectional images by rotating the heading direction. It then determines the current heading direction based on a reference image. Setting the heading direction of the snapshot at the goal location as the reference, the visual compass method offers the current head direction based on comparison of another snapshot with the reference image. When the method is applied in real-world robotic experiments, the images obtained by the omnidirectional camera are compared. However, in this work, we applied the method in a simulation environment. Therefore, the organization of the environmental conditions could affect the performance of the method. In order to effectively apply the visual compass method, appropriate background settings of the simulation environment are required.

Panoramic snapshots taken at the home position at (500, 500) with three types of background settings are shown in Figure 12. While four landmarks are perceived as dark objects (indicated as value 1), the backgrounds have been masked using three different methods. For method 1, a uniform background was allocated as zero, while methods 2 and 3 involve uniform walls and noisy wall allocation, respectively. Method 1 is employed to eliminate any background and leave only the landmarks in the snapshot. Method 2 involves the assignment of a uniform color to background sector images between a pair of landmarks; each sector has its own gray-colored value. The random value shown in method 3 indicates that the background is extremely noisy. The snapshot images taken

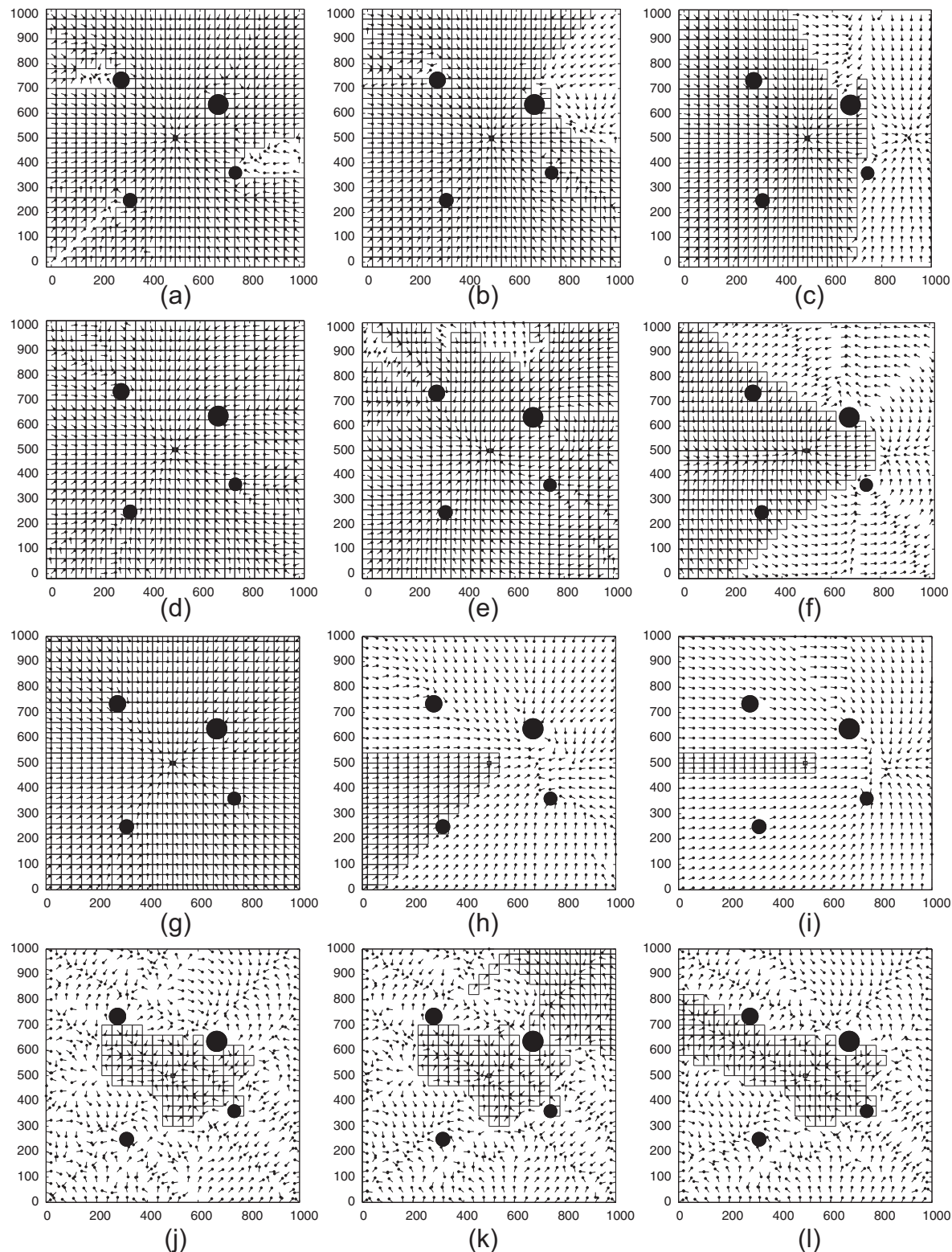


Figure 9. Vector map with the catchment area (boxed region) for (a)–(c) the DELV method with a compass, (d)–(f) the ACV method, (g)–(i) the ALV method and (j)–(l) the GIS method. The number of occluded landmarks is zero for (a), (d), (g) and (j), one for (b), (e), (h) and (k), and two for (c), (f), (i) and (l).

at the home position in the simulation environment after applying methods 1–3 are shown in Figure 12(a)–(c), respectively.

For methods 1, 2 and 3, we assessed the performance of the visual compass method for estimating the heading direction. The estimation of the heading direction

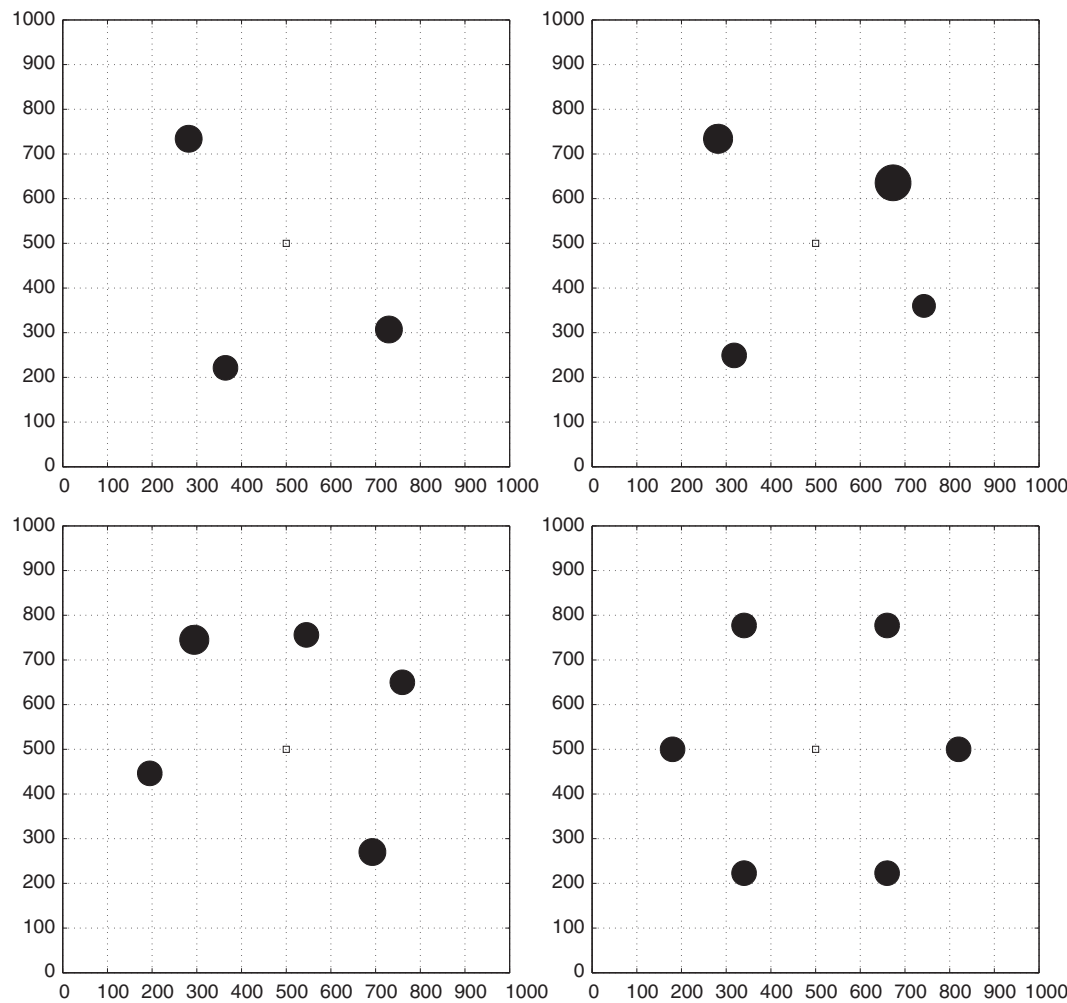


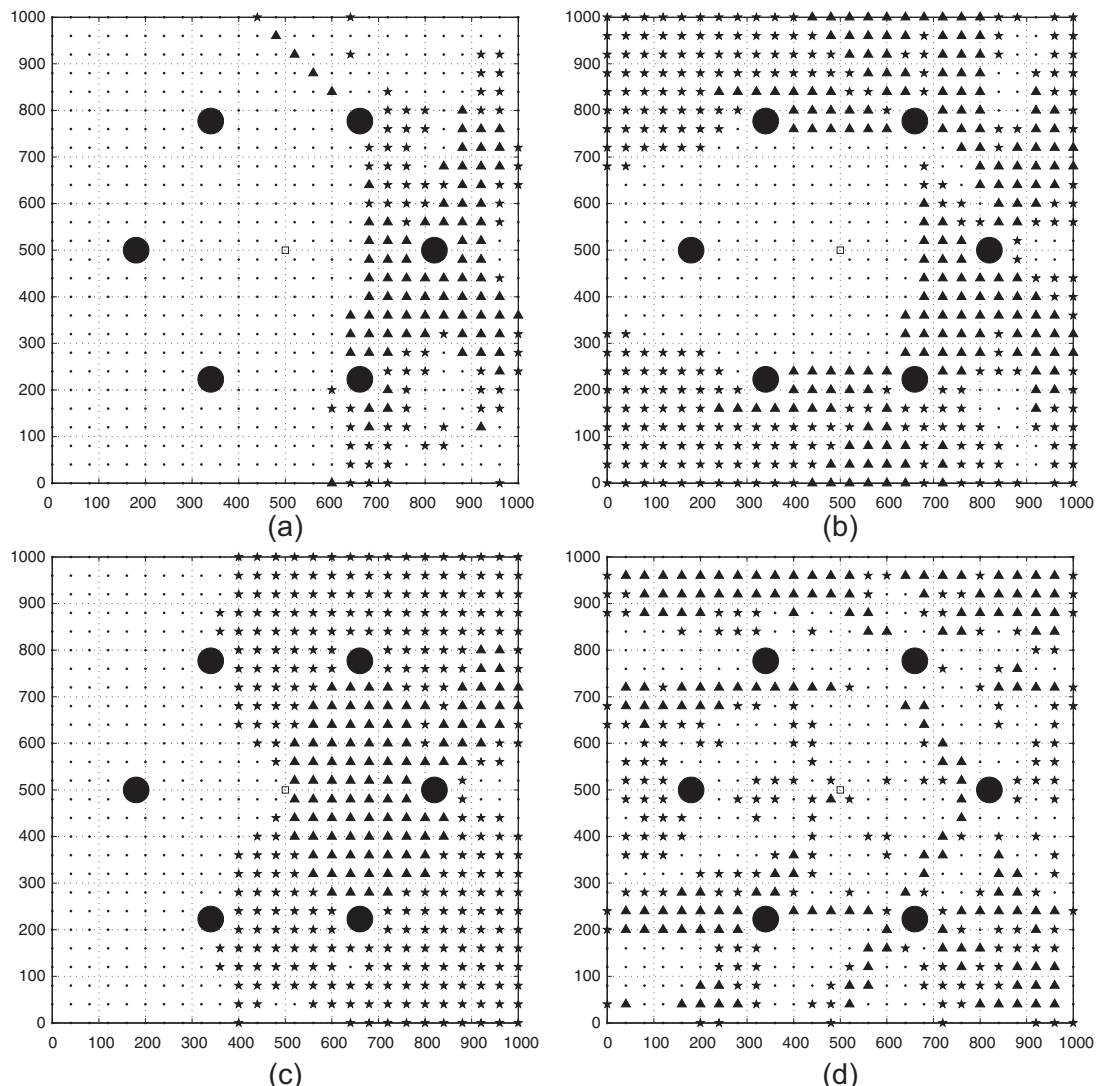
Figure 10. Environments with varying numbers of landmarks for occlusion test.

Table 3. Error point rate (%) for environments with varying landmark numbers (D: DELV method; W: Weber's ACV method; A: ALV method; L: Labrosse's GIS method)

| Occluded # | None | 1 | | 2 | | 3 | |
|------------|------|---------|---------|---------|---------|---------|---------|
| | | e > 45° | e > 90° | e > 45° | e > 90° | e > 45° | e > 90° |
| L = 3 | D | 2.54 | 2.69 | 5.68 | 0.75 | 27.5 | 9.12 |
| | W | 21.67 | 2.09 | 30.64 | 12.11 | 56.05 | 28.25 |
| | A | 1.35 | 0 | 20.33 | 5.83 | 26.46 | 24.51 |
| | L | 32.88 | 15.99 | 29.3 | 9.57 | 24.81 | 5.08 |
| L = 4 | D | 5.73 | 3.02 | 6.79 | 3.62 | 17.04 | 7.54 |
| | W | 9.65 | 0.15 | 25.34 | 7.39 | 52.64 | 27.45 |
| | A | 0.15 | 0 | 18.40 | 3.77 | 42.68 | 10.41 |
| | L | 34.41 | 30.92 | 38.16 | 27.75 | 35.44 | 27.79 |
| L = 5 | D | 6.19 | 7.10 | 8.31 | 4.08 | 12.08 | 8.01 |
| | W | 9.67 | 3.47 | 32.18 | 5.29 | 37.01 | 21.9 |
| | A | 3.17 | 0 | 24.92 | 4.23 | 35.65 | 12.08 |
| | L | 33.99 | 37.76 | 31.72 | 33.38 | 33.84 | 27.64 |
| L = 6 | D | 9.05 | 7.67 | 5.37 | 7.67 | 10.89 | 8.59 |
| | W | 3.68 | 2.15 | 11.2 | 5.52 | 31.29 | 13.8 |
| | A | 0 | 0 | 6.75 | 1.23 | 29.6 | 9.97 |
| | L | 26.23 | 33.59 | 24.87 | 35.58 | 25.31 | 32.52 |

Table 4. Catchment area rate (%) for environments with different landmark numbers

| Occluded # | | None | 1 | 2 | 3 |
|------------|------|-------|-------|-------|-------|
| $L = 3$ | DELV | 94.82 | 100 | 17.46 | - |
| | ACV | 99.56 | 8.28 | 5.62 | - |
| | ALV | 100 | 15.68 | 15.53 | - |
| | GIS | 41.27 | 40.98 | 57.99 | - |
| $L = 4$ | DELV | 92.01 | 85.95 | 63.46 | - |
| | ACV | 100.0 | 93.79 | 46.3 | - |
| | ALV | 100 | 17.6 | 4.14 | - |
| | GIS | 12.87 | 27.07 | 18.93 | - |
| $L = 5$ | DELV | 87.43 | 87.13 | 67.16 | 65.98 |
| | ACV | 91.12 | 85.05 | 54.14 | 52.81 |
| | ALV | 100 | 16.86 | 6.21 | 6.21 |
| | GIS | 9.91 | 9.91 | 13.02 | 10.65 |
| $L = 6$ | DELV | 73.67 | 84.91 | 63.17 | 63.91 |
| | ACV | 99.85 | 94.23 | 61.09 | 39.5 |
| | ALV | 100 | 30.77 | 3.55 | 3.55 |
| | GIS | 27.75 | 15.98 | 17.60 | 22.19 |

**Figure 11.** Environments with six landmarks and angular errors for homing direction; three landmarks are missing in this experiment: (a) DELV method (b) ACV method (c) ALV method and (d) GIS method.

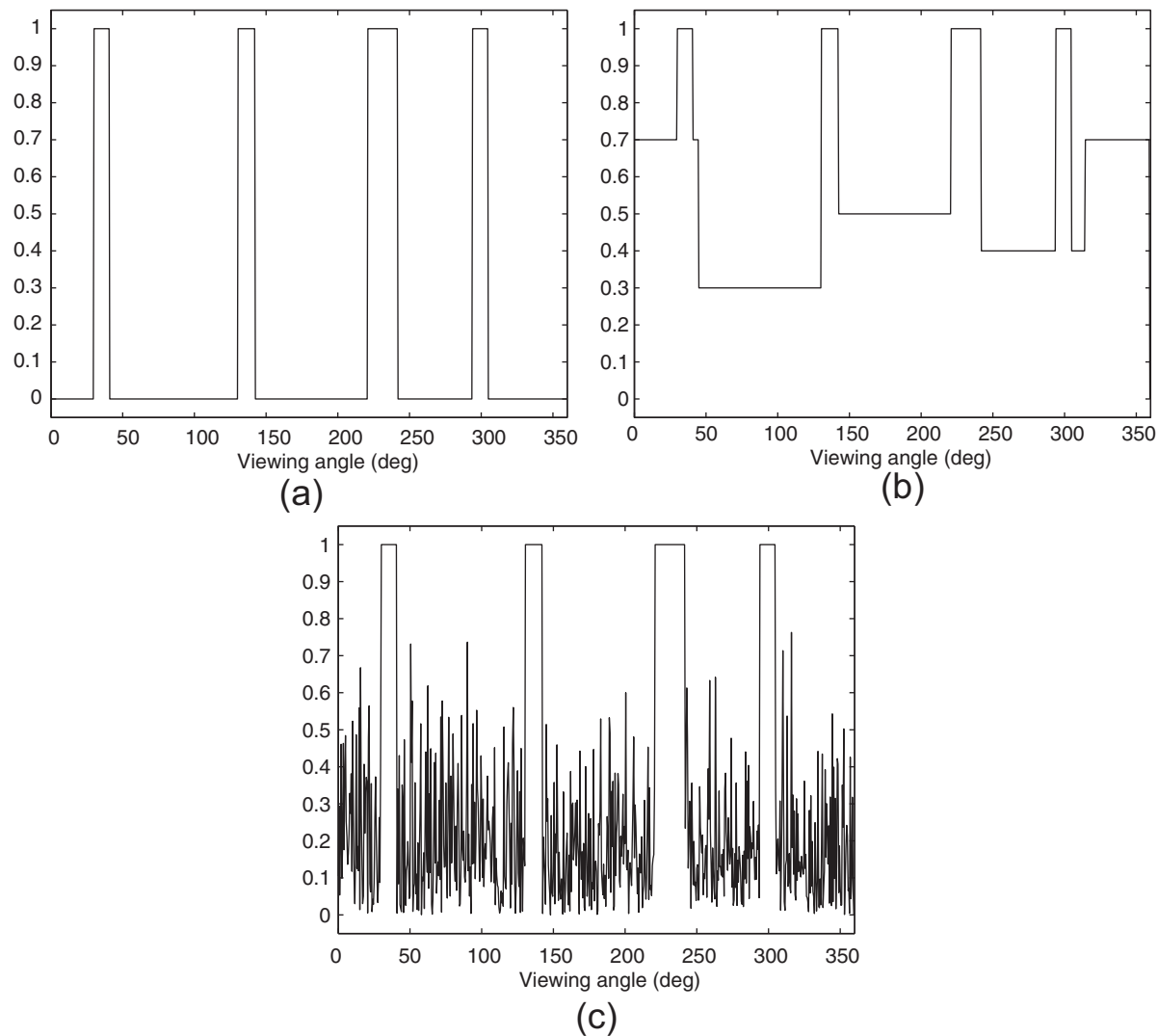


Figure 12. Panoramic snapshot images at (500, 500) after applying different background setting methods: (a) method 1, (b) method 2 and (c) method 3.

for each location in the map is shown in Figure 13. The arrows represent the estimated direction; an accurate result would be an arrow pointing in an upward direction. Based on the vector map results, we can conclude that Figure 13(b) displays the best performance in heading direction estimation. This result is also shown in the error graph in Figure 14. As expected from the vector map results, the error graphs in Figure 14 reveal that the errors are much smaller when method 2 is applied. Based on this result, it can be said that the performance of the visual compass method in simulation is affected by the background settings. For later experiments, method 2 was chosen for the background settings between a pair of landmarks.

4.2 Visual compass experiments

In the previous section, the reference compass information at each point was provided by the DELV and the

ACV models. The DELV algorithm does not necessarily require compass information. However, for a fair comparison with the ACV method, which cannot be operated without a compass, the direction estimation process in the DELV was replaced by assuming the use of a reference compass. In this section, we apply a visual compass instead of reference compass information to the DELV, ACV, and ALV models and analyze the results. The DELV has its own heading direction estimation algorithm, but it is replaced with the estimation obtained with the visual compass method so as to maintain consistency in the experimental conditions.

Shown in Figure 15 are the results obtained with the DELV, ACV, ALV and GIS methods when the compass is estimated with the visual compass method. Since the heading estimation according to the visual compass method does not guarantee accuracy, the results show a somewhat larger error in the direction of the homing vector compared with the results obtained when a

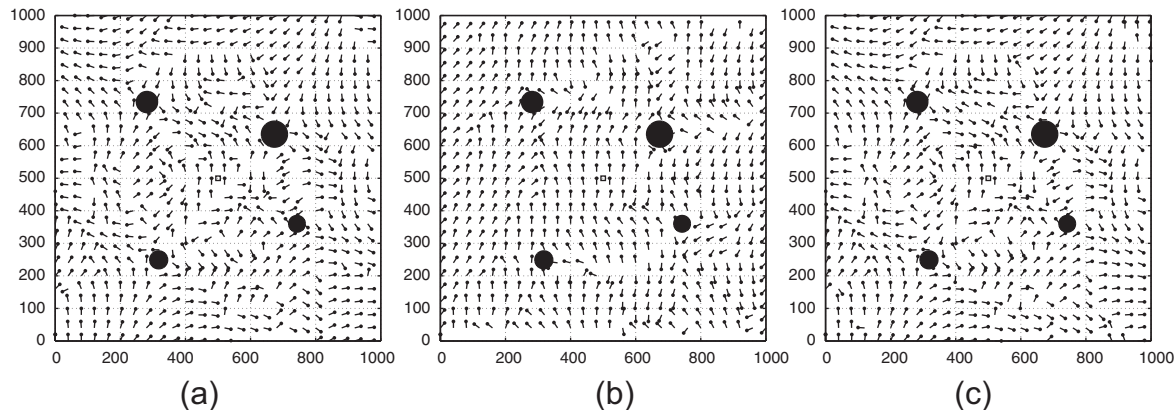


Figure 13. Vector maps indicating the estimated heading directions with the visual compass method obtained with (a) method 1, (b) method 2 and (c) method 3; if the direction is estimated accurately, the resulting arrows should point upward.

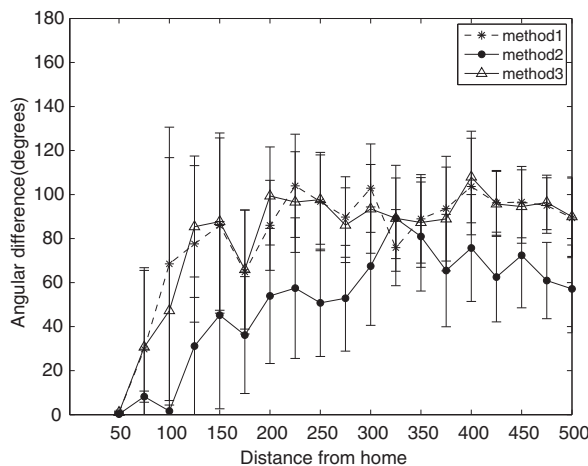


Figure 14. Error graphs of the heading directions with the visual compass approach based on the three different methods.

reference compass is given (see Figure 5). The error graphs are given in Figure 16. With the reference compass and without any missing landmark, the ALV shows the best performance (see Figure 6). However, upon application of the visual compass method, the error of the DELV method is smaller than that of the ALV model, whose error rate is the most increased. This result indicates that the ALV and ACV models are quite dependent on the compass information, and thus the performance of the navigation is vulnerable to the accuracy of the reference compass. Therefore, we can presume that the DELV method is more robust when there is no reference compass information.

Another criterion for evaluating the performances of the navigation methods, a homing path analysis, is shown in Figure 15. Homing path analysis is important since increasing the homing accuracy is the ultimate goal of the navigation algorithms. The catchment area consists of points that could successfully lead to the home location using the decided homing vector. The

squared points in the maps of Figure 15 are the catchment areas; an agent starting from outside these regions will fail to reach home. The sizes of the catchment areas in the maps for the DELV, ACV, ALV and GIS methods are 74.85%, 47.04%, 40.68% and 16.86%, respectively. The reason for the low catchment areas with the ACV and ALV methods seems to be related to an increase in the trap points in the environment. However, it is hard to analyze how many trap points are expected in a given environment, and it can be decided empirically depending on the environment. The low catchment area with Labrosse's GIS method is due to the existence of many trap points in the vector map. Because Labrosse's method largely depends on the small catchment area of these landmark arrangement by the characteristic of this technique and there can be a lot of trap points in the outside of the catchment area.

The results show that the DELV method exhibits robust navigation performance not only with respect to the spatial error rate, but also with regard to the homing path analysis.

5 Discussion

We have shown that the DELV method exhibits more robust performance compared with other image-based navigation methods such as the ACV, ALV and GIS method. While the landmark-based navigation method requires the extraction of landmark information from snapshot images, the results show better performance in terms of spatial errors and success rate of homing. Visual compass navigation (gradient image of space) may yield better performance in a more natural or unstructured environment; however, in a simple environment with particular landmarks, the DELV method produces significantly improved results. We compared landmark vector methods with the GIS method, but a better image warping method has been developed

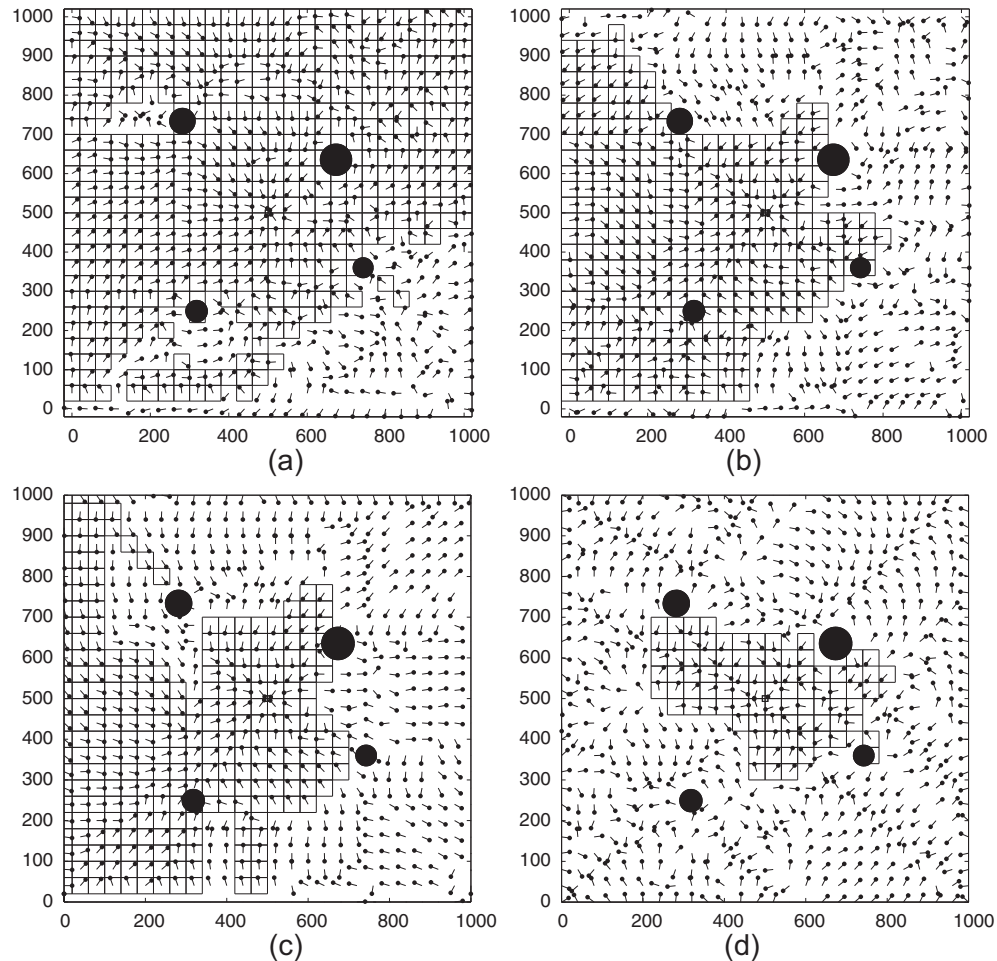


Figure 15. Catchment areas obtained with (a) the DELV, (b) ACV, (c) ALV and (d) GIS methods in combination with the visual compass approach, respectively. The squared points indicate the catchment areas in which the agent could successfully reach the home location by following the decided homing vectors.

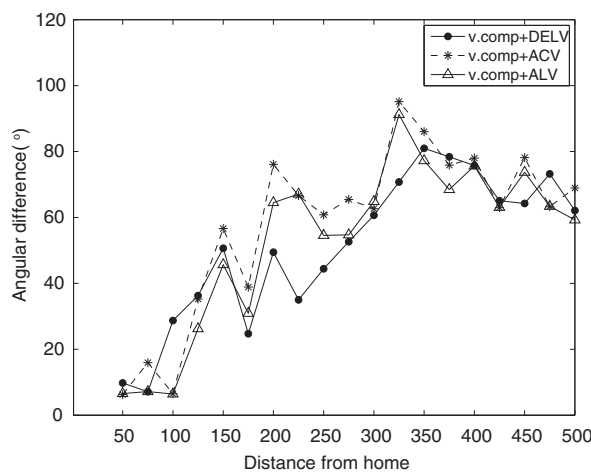


Figure 16. Error graphs obtained from applying the DELV, ACV and ALV methods with the visual compass method.

(Möller & Vardy, 2006) than the GIS. According to their results, it seems that the image warping method is a powerful homing navigation in real environments.

Managing all of the pixel values or pixel difference between a pair of snapshots requires intensive computation time, but the global image processing has an effect of filtering out noise. In contrast, landmark vector methods including the DELV can be sensitive to a decision of landmarks or feature extraction of landmarks. We can compare the landmark vector methods with other image warping methods for more robust homing performance in a natural environment. We leave this for the future work. Here, we have focused on landmark vector methods and explored their performances under occlusions.

In our experiments, we assume that landmarks can be easily discriminated from the background image to focus on the homing algorithm property. In an unstructured environment, we need to select salient features close to the agent as landmark features. The feature extraction process may experience wrong estimation of landmarks or errors in the landmark selection, which has a similar effect to the landmark occlusion. Thus, the above landmark occlusion experiments can

indirectly observe the robustness of the tested algorithms. The results imply that the DELV has a strong potential of homing navigation even in real unstructured environments.

In the experiments, all of the landmarks are cylinder-shaped, but an arbitrary form of landmarks can influence the center position of landmarks when the agent draws landmark vectors. It is expected that this impact may be minor in the decision of homing vector since a distribution of landmark vectors, not a single vector is considered, but we need further study for the impact. The DELV would show good performance if the landmark features are distinguished from the background image. Landmark vector methods are computationally efficient and their search for homing navigation is based on a set of landmarks. A relatively small number of landmarks would have an advantage of less computation time. However, if the feature extraction of landmarks is not successful in a snapshot image (that is, wrong correspondence of landmarks between a pair of snapshots is made), the performance of the DELV method will degrade, depending on the identification level of landmarks. To improve the feature extraction, possibly the correspondence of particular points in an image can be found in another snapshot image with the help of image processing, and those image features could be regarded as landmarks. Then the landmark vector methods could be more effective in real environments. We will test this approach in the future work.

6 Conclusions

In this paper, we analyzed the DELV method in comparison with other landmark-based homing algorithms in various environments. Many homing algorithms have been suggested in previous research. Among these approaches, the ALV and ACV methods are conceptually similar to the DELV method in terms of landmark vectors and difference quantification between landmark vectors. The methods define the angular position of a landmark as the landmark vector and compute the difference between a pair of landmark vectors in one snapshot and in a reference snapshot to obtain the homing vector. We evaluated the performances of the models by analyzing the homing vector and assessing the homing path. The homing vector analysis can yield the performance from a spatial perspective, while the success rate in homing was represented by the size of the catchment area. In experiments with artificial occlusions of the landmarks, the DELV method exhibited a lower rate of error and a larger catchment area in the environment compared with that of the ACV, ALV and the GIS method.

The performances of the methods were also analyzed with no reference compass information. We

instead used a visual compass method that depended purely on snapshot images to estimate the heading orientation since it is known that the visual compass approach is quite robust in robotic experiments. With the implemented approach, the DELV method exhibited better performance than did the ALV, ACV and GIS models. The DELV method combined with the visual compass approach yielded a better catchment area result than did the GIS method with the visual compass approach.

The results described in this paper demonstrate that the DELV method is a robust method that is comparatively less sensitive to the occlusion problem and the accuracy of the heading direction estimation. However, the method has its limitations with regard to return trips to the goal location in some regions or under an increasing number of occlusions. The analysis suggests that an effective navigation algorithm could be obtained using egocentric information. Path integration (Kim & Lee, 2011) or internal memory (Wood, Baxter & Belpaeme, 2012) can guide the agent to an area near the goal after a long-distance journey in the event that too many occlusions are present or when landmarks near the goal are not visible from a long distance. If the agent is finally positioned in the landmark-surrounding zone, the agent can successfully return to the goal. The above approaches solely rely on visual images without any internal state or action-related term, and possibly the sensorimotor map may be helpful to the landmark-based navigation methods (Butz, Shirinov, & Reif, 2010).

The DELV needs the distance information to each landmark. How to encode the landmark vector in a snapshot image would be an interesting issue in the DELV. Possibly the distance information with a laser sensor or other distance sensors could be used instead of visual images for the DELV method. In future research, the overall performance of the DELV method could be improved by compensating for its disadvantages and emphasizing the strong points of previous navigation methods. The method could then be applied to real-world robotic tasks. An alternative technique is to simultaneously apply the three landmark-based algorithms (the DELV, ACV and ALV methods) and vote on the homing directions obtained from each method to determine the direction of movement. This may increase the catchment area from which it is possible to return home. Alternatively, the homing vectors from the three methods can be summed to create an improved homing vector.

Funding

This work was supported by the Basic Science Research Program through a NRF (National Research Foundation of Korea) grant funded by the Ministry of Education, Science and Technology (grant number 2012-0001626).

References

- Baddeley, B., Graham, P., Philippides, A., & Husbands, P. (2011). Holistic visual encoding of ant-like routes: Navigation without waypoints. *Adaptive Behavior*, 19, 3–15.
- Butz, M. V., Shirinov, E., & Reif, K. L. (2010). Self-Organizing Sensorimotor Maps Plus Internal Motivations Yield Animal-Like Behavior. *Adaptive Behavior*, 18, 315–337.
- Cartwright, B., & Collett, T. (1983). Landmark learning in bees. *Journal of Comparative Physiology A*, 151(4), 521–543.
- Cartwright, B., & Collett, T. (1987). Landmark maps for honeybees. *Biological Cybernetics*, 57(1), 85–93.
- Chen, G., & Tsai, W. (1998). An incremental-learning-by-navigation approach to vision-based autonomous land vehicle guidance in indoor environments using vertical line information and multiweighted generalized hough transform technique. *IEEE Transactions on Systems, Man, and Cybernetics, Part B*, 28(5), 740–748.
- Cheng, K., Collett, T., Pickhard, A., & Wehner, R. (1987). The use of visual landmarks by honeybees: Bees weight landmarks according to their distance from the goal. *Journal of Comparative Physiology A*, 161(3), 469–475.
- Collett, M., & Collett, T. (2000). How do insects use path integration for their navigation? *Biological Cybernetics*, 83(3), 245–259.
- Collett, T. (1996). Insect navigation en route to the goal: multiple strategies for the use of landmarks. *Journal of Experimental Biology*, 199(1), 227.
- Esch, H., & Burns, J. (1995). Honeybees use optic flow to measure the distance of a food source. *Naturwissenschaften*, 82(1), 38–40.
- Franz, M., Schölkopf, B., Mallot, H., & Bülthoff, H. (1998). Where did I take that snapshot? Scene-based homing by image matching. *Biological Cybernetics*, 79(3), 191–202.
- Goldhoorn, A., Ramisa, A., Mantaras, R. de, & Toledo, R. (2007). Using the average landmark vector method for robot homing. *Frontiers in artificial intelligence and applications*, 163, 331–338.
- Hafner, V. (2001). Adaptive Homing–Robotic Exploration Tours. *Adaptive Behavior*, 9(3–4), 131–141.
- Hafner, V., & Möller, R. (2001). Learning of visual navigation strategies. In *European workshop on learning robots (ewlr), prague*.
- Hong, J., Tan, X., Pinette, B., Weiss, R., & Riseman, E. (1991). Image-based homing. In *Proc. int. conf. robotics and automation* (pp. 620–625).
- Kim, D., & Lee, J. (2011). Path Integration Mechanism with Coarse Coding of Neurons. *Neural Processing Letters*, 34(3), 277–291.
- Labrosse, F. (2006). The visual compass: performance and limitations of an appearance-based method. *Journal of Field Robotics*, 23(10), 913–941.
- Labrosse, F. (2007). Short and long-range visual navigation using warped panoramic images. *Robotics and Autonomous Systems*, 55(9), 675–684.
- Lambrinos, D., Möller, R., Labhart, T., Pfeifer, R., & Wehner, R. (2000). A mobile robot employing insect strategies for navigation. *Robotics and Autonomous Systems*, 30(1–2), 39–64.
- Luschi, P., Papi, F., Liew, H., Chan, E., & Bonadonna, F. (1996). Long-distance migration and homing after displacement in the green turtle (*Chelonia mydas*): a satellite tracking study. *Journal of Comparative Physiology A*, 178(4), 447–452.
- Mather, J. (1991). Navigation by spatial memory and use of visual landmarks in octopuses. *Journal of Comparative Physiology A*, 168(4), 491–497.
- Möller, R. (2000). Insect visual homing strategies in a robot with analog processing. *Biological Cybernetics*, 83(3), 231–243.
- Möller, R. (2001). Do insects use templates or parameters for landmark navigation? *Journal of Theoretical Biology*, 210(1), 33–45.
- Möller, R. (2009). Local visual homing by warping of two-dimensional images. *Robotics and Autonomous Systems*, 57(1), 87–101.
- Möller, R., & Vardy, A. (2006). Local visual homing by matched-filter descent in image distances. *Biological Cybernetics*, 95(5), 413–430.
- Papi, F. (1990). Olfactory navigation in birds. *Cellular and Molecular Life Sciences*, 46(4), 352–363.
- Rossier, J., Haeberli, C., & Schenk, F. (2000). Auditory cues support place navigation in rats when associated with a visual cue. *Behavioural brain research*, 117(1–2), 209–214.
- Schmudderich, J., Willert, V., Eggert, J., Rebhan, S., Goerick, C., Sagerer, G., et al. (2008). Estimating object proper motion using optical flow, kinematics, and depth information. *IEEE Transactions on Systems, Man, and Cybernetics, Part B: Cybernetics*, 38(4), 1139–1151.
- Smith, L., Philippides, A., Graham, P., Baddeley, B., & Husbands, P. (2007). Linked local navigation for visual route guidance. *Adaptive Behavior*, 15(3), 257–271.
- Stürzl, W., & Zeil, J. (2007). Depth, contrast and view-based homing in outdoor scenes. *Biological Cybernetics*, 96(5), 519–531.
- Tovar, B., Murrieta-Cid, R., & LaValle, S. (2007). Distance-optimal navigation in an unknown environment without sensing distances. *IEEE Transactions on Robotics*, 23(3), 506–518.
- Vidal-Calleja, T., Sanfeliu, A., & Andrade-Cetto, J. (2010). Action selection for single-camera SLAM. *IEEE Transactions on Systems, Man, and Cybernetics, Part B: Cybernetics*, 40(6), 1567–1581.
- Weber, K., Venkatesh, S., & Srinivasan, M. (1999). Insect-inspired robotic homing. *Adaptive Behavior*, 7(1), 65.
- Wehner, R. (1997). The ants celestial compass system: spectral and polarization channels. *Orientation and communication in arthropods*, 145–185.
- Wehner, R., Michel, B., & Antonsen, P. (1996). Visual navigation in insects: coupling of egocentric and geocentric information. *Journal of Experimental Biology*, 199, 129–140.
- Wehner, R., & Räber, F. (1979). Visual spatial memory in desert ants, *Cataglyphis bicolor* (Hymenoptera: Formicidae). *Cellular and Molecular Life Sciences*, 35(12), 1569–1571.
- Wood, R., Baxter, P., & Belpaeme, T. (2012). A review of long-term memory in natural and synthetic systems. *Adaptive Behavior*, 20(2), 81–103.
- Yu, S.-E., & Kim, D. (2011). Landmark vectors with quantized distance information for homing navigation. *Adaptive Behavior*, 19(2), 121–141.
- Zeil, J., Hofmann, M., & Chahl, J. (2003). Catchment areas of panoramic snapshots in outdoor scenes. *Journal of the Optical society of America A*, 20(3), 450–469.